Author Manuscript

Author Manuscript

Author Manuscript

Author Manuscript

HHS Public Access

Author manuscript

JACC Cardiovasc Imaging. Author manuscript; available in PMC 2021 June 01.

Published in final edited form as:

JACC Cardiovasc Imaging. 2020 June ; 13(6): 1368–1383. doi:10.1016/j.jcmg.2019.07.015.

How to Image Cardiac Amyloidosis:

A Practical Approach

Sharmila Dorbala, MD, MPH[a,b,c], **Sarah Cuddy, MB BCh, BAO**[a,b,c], **Rodney H. Falk, MD**[c]

[a]Division of Nuclear Medicine, Department of Radiology, Brigham and Women's Hospital, Boston, Massachusetts

[b]CV Imaging Program, Cardiovascular Division, Brigham and Women's Hospital, Boston, Massachusetts

[c]Cardiac Amyloidosis Program, Division of Cardiology, Department of Medicine, Brigham and Women's Hospital, Boston, Massachusetts.

Abstract

Cardiac amyloidosis (CA) is one of the most rapidly progressive forms of heart disease, with a median survival from diagnosis, if untreated, ranging from <6 months for light chain amyloidosis to 3 to 5 years for transthyretin amyloidosis. Early diagnosis and accurate typing of CA are necessary for optimal management of these patients. Emerging novel disease modifying therapies increase the urgency to diagnose CA at an early stage and identify patients who may benefit from these life-saving therapies. The goal of this review is to provide a practical approach to echocardiography, cardiac magnetic resonance, and radionuclide imaging in patients with known or suspected CA.

Keywords

amyloid tracers; cardiac amyloidosis; cardiac magnetic resonance; CMR; echocardiography; imaging; multimodality; radionuclide imaging; PET; pyrophosphate; Tc-99m–PYP

Cardiac amyloidosis (CA) is one of the most rapidly progressive forms of heart disease, with a median survival from diagnosis, if untreated, ranging from <6 months for light chain amyloidosis (AL) (1) to 3 to 5 years for transthyretin amyloidosis (ATTR) (2). In AL amyloidosis, the amyloid fibrils are derived from immunoglobin light chains (3) produced by a clonal plasma cell disorder, whereas in ATTR amyloidosis, they are formed from the transthyretin protein produced in the liver. ATTR amyloidosis is most commonly from wild-type protein, with associated age-related misfolding (ATTRwt) and less commonly from misfolding of variant TTR in patients with an autosomal dominant TTR gene mutation (ATTRv). Varied clinical manifestations and the perceived rarity of the disease are the current challenges for early diagnosis. For the first time, advances in imaging are revealing a

ADDRESS FOR CORRESPONDENCE: Dr. Sharmila Dorbala, Cardiac Amyloidosis Program, Division of Nuclear Medicine, Department of Radiology, Cardiovascular Division, Department of Medicine, Brigham and Women's Hospital and Harvard Medical School, 75 Francis Street, Boston, Massachusetts 02115. sdorbala@bwh.harvard.edu.

APPENDIX For supplemental tables, please see the online version of this paper.

Author Manuscript Author Manuscript Author Manuscript Author Manuscript

high prevalence of cardiac amyloid deposits in specific populations (4-7). The goal of this review is to provide a practical approach to noninvasive imaging in patients with known or suspected CA.

WHAT IS THE GOLD STANDARD FOR THE DIAGNOSIS OF CA?

Congo red staining of amyloid deposits showing apple-green birefringence under polarized light is the definitive way of determining the presence of amyloid in tissue, but this test does not determine the type of amyloid. Because amyloidosis is a systemic disorder, biopsies can be obtained from several sites, including the heart (in ATTR, due to predominant cardiac involvement), abdominal fat pad, bone marrow (as part of work-up for plasma cell dyscrasia in suspected AL amyloidosis), or kidney (8). Once amyloid deposits are found, typing is most accurately characterized (>98% sensitivity) by mass spectrometry (9) because immunohistochemistry and other previously used techniques can give misleading results (8).

Until recently, CA was only diagnosed by a positive endomyocardial biopsy or a positive extracardiac biopsy in combination with left ventricular (LV) wall thickness >12 mm on echocardiography unexplained by other causes. Although fat pad biopsy and/or aspirate is simple, its yield is lower in diagnosing ATTR (ATTRv: 45%, ATTRwt: 15%) than diagnosing AL (84%) amyloidosis. A degree of expertise is required in finding the limited amyloid deposits (10). Accumulating literature now supports the new notion that typical imaging features on technetium-99m (Tc-99m)–pyrophosphate (PYP)/3, 3-diphosphono-1,2-propanodicarboxylicacid (DPD)/hydroxymethylene diphosphonate (HMDP) imaging can almost definitively diagnose ATTR CA. Endomyocardial biopsy is currently reserved for equivocal imaging findings or in patients with discordant clinical and imaging findings.

WHY IS EARLY DIAGNOSIS AND ACCURATE TYPING OF CA IMPORTANT?

CA is a major predictor of adverse cardiac outcomes in AL amyloidosis. Imaging has the power to identify patients with AL with a higher risk of mortality and can guide the selection of the optimal chemotherapeutic regimen; modulation of the dose of chemotherapy based on imaging findings may mitigate treatment-associated exacerbation of heart failure. In the case of ATTRv gene carriers, and in patients with heart failure with preserved ejection fraction (HFpEF), identification of ATTR CA may allow for initiation of novel targeted antiamyloid therapies (11-13). Hence, early diagnosis of cardiac involvement and typing of fibrils into AL or ATTR are both critical.

WHAT ARE THE CLINICAL PHENOTYPES OF CA?

Heart failure, especially HFpEF, is an early and characteristic feature of CA. These patients may present with a variety of other clinical phenotypes. ATTRwt CA is emerging as 1 of the major specific causes of HFpEF. With progressive amyloid accumulation, the cardiac chambers thicken concentrically (in 68% of patients with AL) or asymmetrically with septal thickening (in 79% of patients with ATTR) (14). LV outflow tract obstruction with increased gradient is occasionally seen and may be misdiagnosed as hypertrophic cardiomyopathy, with deleterious management consequences. A thick ventricle with small cavity size,

Author Manuscript Author Manuscript Author Manuscript Author Manuscript

reduced stroke volume, and fixed cardiac output are features of advanced CA (Figure 1). Similar morphological changes are seen in aortic stenosis, which can coexist with CA. Recent data suggest that ATTR CA is associated with paradoxical low-flow, low-gradient aortic stenosis with mid-range ejection fraction [EF] (mean EF of 48%) (5).

Autonomic and sensorineural neuropathy, and orthostatic hypotension are common features of certain forms of hereditary ATTRv and AL and can be a complication of therapy in patients with AL. The previously discussed structural cardiac changes, combined with ventricular stiffness and autonomic neuropathy, make these individuals highly sensitive to heart rate and volume changes; negative inotropes or vasodilators may predispose them to hypotension and/or collapse (15).

OTHER PHENOTYPES.

Atrial fibrillation is common in amyloidosis, and irregular rhythm is poorly tolerated due to stiff ventricles. Despite amyloid infiltration, the atria dilate because of high LV filling pressures. Atrial amyloid infiltration causes atrial dysfunction and atrial fibrillation. Atrial dysfunction in CA increases the risk of thrombogenicity (16) and stroke, even with normal sinus rhythm (17). Coronary microvascular dysfunction is ubiquitous in AL and ATTR CA (18) and can manifest as angina in the absence of obstructive coronary artery disease. Microvascular dysfunction is not limited to the heart, and occasionally, causes jaw or buttock claudication, particularly in AL amyloidosis (18). Peri-vascular amyloid deposits, as well as autonomic dysfunction (19), may account for microvascular dysfunction, which can be aggravated by thick walls and high LV filling pressure (18).

WHAT ARE THE ADVANTAGES OF IMAGING OVER ENDOMYOCARDIAL BIOPSY IN CA?

Until recently, endomyocardial biopsy has been the reference standard for diagnosing CA; however, it is not widely available. When available, because it is invasive, many cardiologists are hesitant to proceed to biopsy in older adult patients or in patients with early symptoms. Although patients with CA almost always have a positive endomyocardial biopsy, extrapolating the amyloid content on the biopsy sample to the entire heart may be inaccurate, particularly in the early CA when the amyloid deposits may not be extensive or diffuse (20). In contrast, imaging offers substantial advantages. It is widely available, noninvasive, quantitative, provides whole heart imaging to estimate cardiac amyloid burden, and can be easily and successfully repeated to assess response to therapy.

WHAT ARE THE IMAGING TARGETS IN CA?

Amyloid deposits are the most direct target to diagnose and type CA (Central Illustration). The integral components of amyloid include insoluble β-pleated sheets of fibrils formed from misfolded precursor proteins, as well as nonfibrillar components of serum amyloid P component (a glycoprotein) (21), proteoglycans, and other proteins. Iodine-123–labeled serum amyloid P (used currently for systemic AL amyloidosis, but not CA, in the United Kingdom) (21) and Tc-99m–aprotinin (22) (no longer used clinically) are single-photon

Author Manuscript Author Manuscript Author Manuscript Author Manuscript

emission computed tomography tracers that specifically target the amyloid fibril, but are not available in the United States. Tc-99m–PYP, DPD, or HMDP are now recognized as specific markers of ATTR CA (23). Although a calcium-mediated mechanism has been suggested, their mechanism of uptake is poorly understood (24). Amyloid-binding positron emission tomography (PET) tracers (C-11–PiB, F-18–florbetapir, F-18–florbetaben, F-18–flutemetamol), which have been approved by the Food and Drug Administration for imaging Alzheimer's disease, have been successfully used to image AL and ATTR CA, but they are off-label research applications and not approved by the Food and Drug Administration for CA (25-27). These PET tracers are structurally similar to thioflavin-T, with a proposed binding site in the long axis of the β-pleated sheet structure of the amyloid fibril, which may explain their ability to image amyloid independent of precursor proteins (28).

Amyloidosis is characterized by remodeling of the extracellular matrix (29), expansion of extracellular volume (ECV) (30), rarefaction of capillary density, possible edema (31), changes in cardiomyocyte size and/or volume (potentially differentially in AL and ATTR) (32), and eventual gross changes in cardiac structure and function with increased LV mass and wall thickness (33). These indirect markers and/or consequences of CA can be imaged with echocardiography or CMR. The electrocardiogram in myocardial hypertrophy may manifest high voltage, but in CA, electrocardio-graphic voltage may be decreased, normal, or even increased. Traditionally, amyloid deposits were believed to be inert, but several lines of evidence (34) indicate that toxic interactions of AL amyloid fibrils with circulating light chains may account for cellular damage (light chain toxicity). However, methods to image light chain toxicity in the heart are currently lacking.

Quantification of amyloid burden is currently based on evaluation of LV mass, wall thickness, ECV, or semi-quantitative metrics on amyloid PET tracer imaging.

HOW DO YOU USE IMAGING IN CA?

Due to the unique insights provided by each of the imaging tests into the pathogenesis and functional effects of amyloid deposits, patients often need to undergo >1 test for a complete evaluation. In the next few sections, we discuss the typical imaging features of CA on echocardiography, cardiac magnetic resonance (CMR), and radionuclide imaging.

ECHOCARDIOGRAPHY.

Echocardiography is usually the first test performed in patients presenting with heart failure. However, typical echocardiographic features of CA (Figures 1A to 1C) are most prominent in advanced disease (Figures 2A to 2D) and may be missed in earlier disease, even when severe enough to cause heart failure. Particularly in early disease, echocardiography lacks specificity to precisely distinguish amyloid from non-amyloid infiltrative or hypertrophic heart diseases. Nevertheless, it is an extremely useful test, although it requires both a good quality study and an index of suspicion from the interpreting physician for optimal value (Figure 3).

Echocardiography defines the effects of amyloid burden by imaging wall thickness, mass, and chamber dimensions. LV thickness and mass are higher in patients with ATTRwt CA,

Author Manuscript Author Manuscript Author Manuscript Author Manuscript

which likely reflects longer duration of amyloid accumulation compared with AL CA or ATTRv CA (Supplemental Table 1) (33). Despite lower LV mass in AL CA, patients with AL manifest significant diastolic dysfunction, similar to patients with ATTR CA (33). The typical increased myocardial echogenicity described in CA (35) is neither specific nor sensitive for amyloidosis (36).

Echocardiography provides exclusive insights on diastolic function and LV filling pressures. Low Ewave and high A-wave velocity, decreased E/A ratio, and normal deceleration time are markers of early disease, whereas a normal E wave, small A wave, high E/A ratio, a rapid deceleration time on diastolic mitral valve inflow (restrictive pattern of LV filling), and small S-wave pulmonary venous spectral Doppler patterns indicate advanced disease (Figure 1B) (37). On tissue Doppler imaging, the mitral and tricuspid annular e′ velocities are markedly reduced, with a high E/e′ ratio indicating high filling pressures (38). These features usually manifest after an obvious increase in wall thickness, but occasionally may be evident even before an overt increase in LV wall thickness.

In CA, LVEF is typically preserved until late stages (33,37), but longitudinal LV contraction is impaired early in the disease. Stroke volume is often reduced (33) and portends poor survival in AL CA (39). Changes in myocardial deformation measured on 2-dimensional speckle tracking imaging are prevalent in CA (93% to 100%) (33). Global longitudinal strain is significantly reduced in CA even when LVEF is normal. AL CA, compared with ATTR-CA, is characterized by worse strain values at a given level of wall thickness, which supports the light chain toxicity hypothesis (33). A regional pattern of strain with severe impairment of strain at the mid and basal segments and relative apical sparing of longitudinal strain (a ratio of apical longitudinal strain/average of longitudinal strain in the mid and basal myocardial segments >1.0) is sensitive (93%) and specific (82%) to distinguish CA from LV hypertrophy (40). The reasons for this phenomenon are not known. Smaller amyloid deposition in the apical segments (in ATTR CA) (41) and regional differences in total amyloid mass in the apical segments compared with the mid and basal segments (in AL CA) have been proposed (42). Abnormal global longitudinal strain is an independent predictor of poor survival in both forms of CA (33,43,44).

Unexplained right ventricular thickening and systolic dysfunction is another clue for amyloidosis. In AL CA, systolic strain of the basal segment of the right ventricular free wall and tricuspid annular plane systolic excursion identified patients with early impairment of right ventricular longitudinal systolic function and worse prognoses (45,46). Right ventricular dilation also portends worse prognosis (47).

Bi-atrial enlargement is common in CA, and a small A wave on mitral inflow Doppler, particularly in the absence of other features of restrictive LV filling, is a clue to atrial dysfunction. In our experience, this finding on echocardiography is associated with a risk of thromboembolism, despite sinus rhythm; we consider using anticoagulation in these patients. Left atrial reservoir and pump function on strain imaging are significantly impaired, regardless of left atrial volume and LVEF in ATTR CA (48). Left atrial peak longitudinal strain (reservoir function) and active emptying fraction (active function) are lower in patients with ATTRwt compared with patients with AL and ATTRv (49).

Author Manuscript Author Manuscript Author Manuscript Author Manuscript

Small pericardial or pleural effusions can be frequently appreciated; in the context of thickened ventricles and restrictive filling, these findings should raise the suspicion for CA.

CMR.

CMR provides high definition structural imaging and tissue characterization that are often incremental to information obtained on echocardiography. In amyloidosis, the intrinsic signal of the myocardium can be measured using T1-/T2-weighted imaging sequences, T1 mapping (pre- and/or post-contrast), late gadolinium enhancement (LGE), and ECV imaging. These markers, although pathognomonic in patients with biopsy-proven amyloidosis, are not specific for amyloidosis and can be elevated in other forms of cardiovascular disease, including reactive or replacement fibrosis and inflammation. CMR can be limited in patients with atrial fibrillation, limited cooperation due to repetitive breath holds, advanced renal dysfunction that limits use of gadolinium, and non-compatible intracardiac devices (although data now support CMR use in some of these patients). Despite these limitations, the unique strengths of CMR have been successfully leveraged in CA as illustrated in Figures 4A to 4C. Supplemental Table 2 shows the range of published myocardial parameters by CMR in patients with AL and ATTR CA (33).

LGE.

LGE using gadolinium-based contrast agents is the cornerstone technique for the diagnosis of CA. Traditional LGE imaging techniques require an operator-determined null point, which is the inversion recovery time at which the normal myocardium appears black or “nulled.” This can be challenging in CA, and difficulty nulling the myocardium or myocardial nulling before blood pool (on TI scout sequence) is strongly suggestive of CA with high sensitivity (100%) (50). The development of a phase-sensitive inversion recovery sequence has made LGE imaging less operator-dependent. Global subendocardial enhancement, transmural LGE, and to a lesser degree, a focal, patchy LGE, are all features of CA (51,52), with a sensitivity of 86% and specificity of 92% (53). LGE is highly prevalent (100% LGE in LV and 96% LGE in right ventricle) and more common in ATTR than AL CA but cannot distinguish between subtypes of CA (14). LGE is a significant predictor of mortality in AL, ATTRv, and ATTRwt ($p < 0.001$) (52), and in patients with transmural LGE, overall survival at 24 months is worse for AL (45%) than for ATTR CA (65%). A limitation of LGE is that it is not easily quantifiable, especially in amyloidosis, which makes it unreliable for tracking changes over time. The newer quantitative technique of T1 mapping can overcome this limitation and potentially detect amyloid infiltration earlier in the disease process than LGE.

T1 MAPPING AND ECV BY CMR.

T1 mapping measures the T1 signal of each pixel and/or voxel in an image. Native T1 values (pre-gadolinium contrast) are higher in areas of amyloid deposition (or diffuse fibrosis) compared with normal tissues. In contrast to ECV, which characterizes the extracellular space, the native T1 values provide a combined signal from myocyte and extracellular space and reflect changes in either or both of those tissue compartments. Native T1 is markedly increased in CA (54) and correlates well with markers of systolic and diastolic dysfunction (55), with 92% sensitivity and 91% specificity to detect CA (55). It identified early

Author Manuscript Author Manuscript Author Manuscript Author Manuscript

amyloidosis in ATTRv gene carriers without LGE (54). Native T1 is valuable in patients with contraindications to gadolinium, including the 30% of patients with AL and ATTR CA with renal dysfunction. However, a major limitation of native T1 is the lack of reproducibility for different scanners or magnetic field strengths (1.5-T vs. 3.0-T). Its independent prognostic value over other risk markers has not been definitively demonstrated (56,57).

Post-contrast T1 mapping and ECV estimation are performed following gadolinium administration, with ECV being more reproducible than absolute T1 values (58). The ECV values are markedly elevated in CA and correlate with other markers of CA severity (30), but do not distinguish between the subtypes of CA. However, ECV has provided insight into myocardial response to amyloid deposition; total myocyte cell volume, derived from ECV and indexed LV myocardial volume, was higher in ATTR than AL CA, suggesting concomitant and potentially compensatory myocyte hypertrophy, which might even be protective (32). As a marker of prognosis, ECV is more robust compared with native or post-contrast T1 mapping alone (56). Quantification of ECV offers potential for tracking disease burden and response to therapy, as demonstrated in AL CA (59); more prospective studies are required. ECV is an earlier marker of cardiac involvement in patients with biopsy-proven amyloidosis, but in the absence of biopsy proof, there is overlap in ECV values with other cardiomyopathic pathologies that may limit its specificity to detect early amyloidosis (60).

T2 MAPPING OF EDEMA.

Parametric sequences to measure myocardial T2 relaxation times have not been as extensively evaluated in CA compared with native T1 values or ECV. A recent study showed greater edema and/or T2 relaxation times in 256 patients with amyloidosis compared with 30 control subjects and in treatment-naive AL compared with treatment of AL and ATTR (31). However, there was substantial overlap in mean T2 values between the groups, precluding its use to differentiate between amyloid types or amyloid from healthy control subjects. T2 measures are also more variable than native T1 measures (61).

RADIONUCLIDE MOLECULAR IMAGING.

Cardiac scintigraphy with bone-avid SPECT radiotracers.—Myocardial uptake of Tc-99m–labeled bone-avid radiotracer imaging has long been recognized to represent CA. Despite high initial interest, studies from 20 years ago demonstrated variable diagnostic accuracies for detection of CA. In retrospect, this was likely because those studies included patients with both AL and ATTR CA. Subsequently, in the 2000s, the high specificity of these tracers for ATTR was recognized in the study by Rapezzi et al. (62), which led to widespread clinical adoption.

ATTR CA, a diagnosis that once often required endomyocardial biopsy, can now be diagnosed non-invasively using Tc-99m–PYP/DPD/HMDP imaging. This discovery has transformed clinical practice and research. ATTR CA can be diagnosed at institutions with limited access to endomyocardial biopsy and in patients who decline or who are not candidates for invasive procedures. Patients diagnosed by imaging benefitted from participation in clinical trials of novel ATTR therapies (11-13) at the same time new drug

Author Manuscript Author Manuscript Author Manuscript Author Manuscript

development significantly accelerated. Noninvasive screening for ATTR CA in patients with a variety of clinical presentations, such as HFpEF (4,63), transcatheter aortic valve replacement (5), and carpal tunnel syndrome (6), has become possible. These advances have not only improved disease detection but are providing rare insights into the pathogenesis of ATTR CA that were not previously feasible.

Bone-avid radiotracer imaging provides incremental value to echocardiography and CMR because these modalities distinguish ATTR CA from other forms of heart diseases with LV thickening (23). However, bone-avid radiotracer images lack structural and hemodynamic information, and are typically used in conjunction with echocardiography or CMR. Currently, Tc-99m–DPD/HMDP in Europe and Tc-99m–PYP in the United States are successfully used in the evaluation of ATTR CA. Tc-99m methylene diphosphonate is the most commonly used radiotracer for bone scanning in the United States, but this tracer has low sensitivity for ATTR CA (62). If ATTR CA is suspected in a patient with a recent negative bone scan, the Tc-99m–PYP scan should be repeated.

Tc-99m–PYP/DPD/HMDP images are typically evaluated using a visual grading or semi-quantitative metrics (Figures 5A to 5D, Supplemental Table 3). A visual grade of 0, 1, 2, and 3 indicates no myocardial uptake, or uptake less than, equal to, and greater than rib uptake, respectively. Although initial studies demonstrated high sensitivity and specificity (100%) for Tc-99m–DPD to diagnose ATTR CA, subsequent studies (23) found that >1 in 5 patients with AL CA may demonstrate grade 2 or 3 myocardial uptake of Tc-99m–PYP/DPD/HMDP. Semi-quantitative evaluation using Tc-99m–PYP planar imaging, a heart to contralateral lung uptake (H/CL) ratio of >1.5 at 1 h accurately distinguished ATTR from AL CA with 97% sensitivity and 100% specificity (with a slightly lower specificity in a later multicenter study) (64). Likewise, a high whole body retention of Tc-99m–DPD at 3 h (62) is highly sensitive and specific for ATTR CA. In a recent multicenter publication (64), visual score and H/CL ratio on 1-h imaging were more sensitive and less specific compared with those metrics at 3-h imaging, with similar overall accuracy to diagnose ATTR CA. These investigators proposed a >1.3 ratio for detection of ATTR CA on the 3-h planar images. The semi-quantitative metrics of H/CL and high whole body ratios, unlike the visual score of 0 to 3, were independently predictive of survival (64,65).

A large multicenter study by Gillmore et al. (23) assessed diagnostic accuracy of all 3 tracers, Tc-99m–DPD, Tc-99m–PYP, or Tc-99m–HMDP, in 1,217 patients with suspected CA. Any myocardial radiotracer uptake (grades 1, 2, and 3) was >99% sensitive and 86% specific for detecting ATTR CA, with false positives mostly occurring in patients with AL amyloidosis (77 of 96). Grades 2 or 3 myocardial radiotracer uptake and the absence of a monoclonal protein in serum or urine had a specificity and positive predictive value for ATTR CA of 100%, albeit with a significant drop in sensitivity (70%). These investigators concluded that “cardiac ATTR amyloidosis can be reliably diagnosed in the absence of histology provided that *all of the following conditions are met*: heart failure with echocardiogram or CMR findings consistent with or suggesting amyloidosis, grade 2 or 3 cardiac uptake on radionuclide scintigraphy with ^{99m}Tc-PYP, -DPD, or -HMDP, and absence of detectable monoclonal proteins despite serum immunofixation, urine immunofixation and

Author Manuscript Author Manuscript Author Manuscript Author Manuscript

serum free light chain assay. Histological confirmation and typing should be sought in all cases of suspected CA where these conditions are not met.” (23).

The use of bone tracer cardiac scintigraphy to screen for ATTR CA in specific populations has already yielded interesting insights. ATTR CA is diagnosed by Tc-99m–PYP/DPD/HMDP imaging in 13.3% of older adult patients hospitalized with HFpEF (4), in 16% of patients who are undergoing transcatheter aortic valve replacement (5), and in 10% of patients with carpal tunnel syndrome (6).

TARGETED IMAGING OF CA

Molecular imaging using amyloid-binding PET tracers allows direct detection of amyloid fibrils. A growing body of work has demonstrated the usefulness of C-11–Pittsburgh compound-B, F-18–florbetapir (26,66,67), and F-18–florbetaben (27) in the diagnosis of CA. These PET tracers provide an unprecedented opportunity to specifically image and quantify global and regional amyloid burden in the heart, and to detect molecular changes in the fibril composition, which is an early signal of response to therapy. These PET images have been assessed visually or using 1 of several indexes of myocardial tracer uptake: target-to-background ratio, myocardial retention index, and myocardial standardized uptake value (25-27,66-68).

Antoni et al. (25) demonstrated visual uptake of tracer and a higher retention index of C-11–Pittsburgh compound-B in all patients with AL and ATTR compared with control subjects, but patients with AL could not be distinguished from patients with ATTR. These initial findings were confirmed by other groups (25,68,69). Initial reports suggested that Tc-99m–DPD imaging could be negative despite cardiac amyloid deposition diagnosed by C-11–Pittsburgh compound-B in certain forms of hereditary CA (substitution of single amino acid valine for methionine at position 30 of the TTR gene, V-30M) (69). The requirement for an onsite cyclotron for production of C-11–Pittsburgh compound-B, due to its short half-life of 20 min, limits its use.

Florbetapir is a stilbene derivative that demonstrates high affinity and specificity for amyloid β; it has favorable pharmacokinetics and a longer half-life (109 min) that allows for unit dose delivery to sites without a cyclotron (70). F-18–florbetapir uptake colocalized remarkably well to AL and ATTR amyloid deposits in autopsy-derived myocardial tissue ex vivo (71) and also proved to be both sensitive and specific for detection of CA in vivo (26,27). The myocardial retention index tended to be higher in subjects with AL than in subjects with ATTR but none of the indexes tested (retention index, LV myocardial standardized uptake value, target-to-background ratio, or LV myocardium to liver standardized uptake value ratio) clearly distinguished AL from ATTR CA (26). Similarly, F-18–florbetaben was also unable to differentiate between AL and ATTR CA (27).

Importantly, these tracers provide the ability to image cardiac and systemic amyloid deposits throughout the whole body in AL amyloidosis (Figures 6A to 6C) (66,72). Although they are currently not being used in clinical practice, these amyloid PET radiotracers are being investigated for early detection, quantitation, and assessment of response to therapy.

Author Manuscript Author Manuscript Author Manuscript Author Manuscript

WHEN TO CONSIDER IMAGING FOR CA?

Figure 7 shows an algorithmic approach to imaging-based diagnosis of CA. Most patients with new-onset heart failure benefit from echocardiography and/or CMR to evaluate for etiology of heart failure. However, if clinical suspicion of ATTR CA is high or if CMR or gadolinium are contraindicated (due to devices or renal dysfunction, respectively), Tc-99m–PYP/DPD/HMDP scintigraphy may offer incremental value over CMR. The diagnostic accuracy of Tc-99m–PYP/DPD/HMDP to identify early cardiac amyloid deposits in individuals without heart failure or without typical echocardiographic and/or CMR features of amyloidosis needs further study. Also, with the availability of approved disease-modifying therapeutic options for ATTR CA (11) and emerging data suggesting underdiagnosis of CA (73), evaluation for ATTR-CA could be considered in most individuals with HFpEF aged older than 65 years, but the cost effectiveness of this approach needs further study.

HOW TO USE IMAGING TO ASSESS AMYLOIDOSIS PROGRESSION AND RESPONSE TO THERAPY?

Imaging is a powerful tool to temporally track progression or regression of amyloid burden in the entire heart and its effects on cardiac function (59,74). Successful therapy for CA should ideally reverse amyloid deposits and associated changes in the extracellular matrix and cardiomyocytes, as well as structure and function of the heart. Several recent phase 3 trials of effective drug therapies stabilized ATTR (11) or curtailed the production of ATTR (12,13). Post hoc analyses from 1 of these trials showed a modest improvement in LV structure and function on echocardiography in the treatment group, from baseline to after 18 months of therapy with patisiran (LV wall thickness: mean decrease -0.9 ± 0.4 mm; $p = 0.017$; global longitudinal strain: mean decrease $-1.4 \pm 0.6\%$; $p = 0.015$), and not with placebo (75). In a small study, serial scanning with Tc-99m–PYP, as anticipated from radiotracer properties, was not helpful to evaluate disease progression in advanced ATTR CA (76). More studies are needed to evaluate the role of imaging in assessment of response to therapy.

CONCLUSIONS

Early diagnosis and typing of CA is critical for optimal management of these patients. Emerging disease-modifying therapies increase the urgency to diagnose it at an early stage and identify patients who may benefit from these life-saving therapies. Imaging plays a central role to identifying CA, quantifying disease burden, and guiding management.

Supplementary Material

Refer to Web version on PubMed Central for supplementary material.

Acknowledgments

Drs. Dorbala and Falk are supported by a National Institutes of Health RO1 grant (RO1 HL 130563). Dr. Dorbala is supported by an American Heart Association Grant (AHA 16 CSA 2888 0004); has received consulting fees from

Author Manuscript Author Manuscript Author Manuscript Author Manuscript

GE Health Care, Proclara, and AAA; and has received consulting fees and grant support from Pfizer. Dr. Falk has received consulting fees from Ionis Pharmaceuticals and Alnylam Pharmaceuticals; and has received research funding from GlaxoSmithKline. Dr. Cuddy has reported that she has no relationships relevant to the contents of this paper to disclose.

ABBREVIATIONS AND ACRONYMS

AL	light chain amyloidosis
ATTR	transthyretin amyloidosis
ATTRv	transthyretin amyloidosis gene mutation
ATTRwt	transthyretin amyloidosis wild type
CA	cardiac amyloidosis
CMR	cardiac magnetic resonance
DPD	3,3-diphosphono-1,2-propanodicarboxylicacid
ECV	extracellular volume
EF	ejection fraction
H/CL	heart to contralateral lung uptake
HMDP	hydroxymethylene diphosphonate
HFpEF	heart failure with preserved EF
LGE	late gadolinium enhancement
LV	left ventricular
PYP	pyrophosphate
Tc-99m	technetium-99m

REFERENCES

1. MerLini G, PaLLadini G. Light chain amyloidosis: the heart of the problem. HaematoLogica 2013;98:1492–5. [PubMed: 24091927]
2. Ruberg FL, Berk JL. Transthyretin (TTR) cardiac amyloidosis. Circulation 2012;126:1286–300. [PubMed: 22949539]
3. Glenner GG, Terry W, Harada M, Isersky C, Page D. Amyloid fibril proteins: proof of homology with immunoglobulin Light chains by sequence analyses. Science 1971;172:1150–1. [PubMed: 4102463]
4. Gonzalez-Lopez E, Gallego-Delgado M, Guzzo-Merello G, et al. Wild-type transthyretin amyloidosis as a cause of heart failure with preserved ejection fraction. Eur Heart J 2015;36:2585–94. [PubMed: 26224076]
5. Castano A, Narotsky DL, Hamid N, et al. Unveiling transthyretin cardiac amyloidosis and its predictors among elderly patients with severe aortic stenosis undergoing transcatheter aortic valve replacement. Eur Heart J 2017;38:2879–87. [PubMed: 29019612]
6. Sperry BW, Reyes BA, Ikram A, et al. Tenosynovial and cardiac amyloidosis in patients undergoing carpal tunnel release. J Am Coll Cardiol 2018;72:2040–50. [PubMed: 30336828]

Author Manuscript Author Manuscript Author Manuscript Author Manuscript

7. Castano A, Bokhari S, Maurer MS. Unveiling wild-type transthyretin cardiac amyloidosis as a significant and potentially modifiable cause of heart failure with preserved ejection fraction. Eur Heart J 2015;36:2595–7. [PubMed: 26224073]
8. Sipe JD, Benson MD, Buxbaum JN, et al. Amyloid fibril proteins and amyloidosis: chemical identification and clinical classification. International Society of Amyloidosis 2016 Nomenclature Guidelines. Amyloid 2016;23:209–13. [PubMed: 27884064]
9. Vrana JA, Gamez JD, Madden BJ, Theis JD, Bergen HR 3rd., Dogan A. Classification of amyloidosis by laser microdissection and mass spectrometry-based proteomic analysis in clinical biopsy specimens. Blood 2009;114:4957–9. [PubMed: 19797517]
10. Quarta CC, Gonzalez-Lopez E, Gilbertson JA, et al. Diagnostic sensitivity of abdominal fat aspiration in cardiac amyloidosis. Eur Heart J 2017;38:1905–8. [PubMed: 28605421]
11. Maurer MS, Schwartz JH, Gundapaneni B, et al. Tafamidis treatment for patients with transthyretin amyloid cardiomyopathy. N Engl J Med 2018;379:1007–16. [PubMed: 30145929]
12. Benson MD, Waddington-Cruz M, Berk JL, et al. Inotersen treatment for patients with hereditary transthyretin amyloidosis. N Engl J Med 2018;379:22–31. [PubMed: 29972757]
13. Adams D, Gonzalez-Duarte A, O'Riordan WD, et al. Patisiran, an RNAi therapeutic, for hereditary transthyretin amyloidosis. N Engl J Med 2018;379:11–21. [PubMed: 29972753]
14. Martinez-Naharro A, Treibel TA, Abdel-Gadir A, et al. Magnetic resonance in transthyretin cardiac amyloidosis. J Am Coll Cardiol 2017;70:466–77. [PubMed: 28728692]
15. Falk RH. Diagnosis and management of the cardiac amyloidoses. Circulation 2005;112:2047–60. [PubMed: 16186440]
16. El-Am EA, Dispenzieri A, Melduni RM, et al. Direct current cardioversion of atrial arrhythmias in adults With cardiac amyloidosis. J Am Coll Cardiol 2019;73:589–97. [PubMed: 30732713]
17. Dubrey S, Pollak A, Skinner M, Falk RH. Atrial thrombi occurring during sinus rhythm in cardiac amyloidosis: evidence for atrial electromechanical dissociation. Br Heart J 1995;74:541–4. [PubMed: 8562243]
18. Dorbala S, Vangala D, Bruyere J Jr., et al. Coronary microvascular dysfunction is related to abnormalities in myocardial structure and function in cardiac amyloidosis. J Am Coll Cardiol HF 2014;2:358–7.
19. Migrino RQ, Truran S, Gutterman DD, et al. Human microvascular dysfunction and apoptotic injury induced by AL amyloidosis light chain proteins. Am J Physiol Heart Circ Physiol 2011;301:H2305–12. [PubMed: 21963839]
20. Haq M, Pawar S, Berk JL, Miller EJ, Ruberg FL. Can 99m-Tc-pyrophosphate aid in early detection of cardiac involvement in asymptomatic variant TTR amyloidosis? J Am Coll Cardiol Img 2016;10:713–4.
21. Hawkins PN, Lavender JP, Pepys MB. Evaluation of systemic amyloidosis by scintigraphy with 123I-labeled serum amyloid P component. N Engl J Med 1990;323:508–13. [PubMed: 2377176]
22. Aprile C, Marinone G, Saponaro R, Bonino C, Merlini G. Cardiac and pleuropulmonary AL amyloid imaging with technetium-99m labelled aprotinin. Eur J Nucl Med 1995;22:1393–401. [PubMed: 8586084]
23. GiLLmore JD, Maurer MS, Falk RH, et al. Nonbiopsy diagnosis of cardiac transthyretin amyloidosis. Circulation 2016;133:2404–12. [PubMed: 27143678]
24. Pepys MB, Dyck RF, de Beer FC, Skinner M, Cohen AS. Binding of serum amyloid P-component (SAP) by amyloid fibrils. Clin Exp Immunol 1979;38:284–93. [PubMed: 118839]
25. Antoni G, Lubberink M, Estrada S, et al. In vivo visualization of amyloid deposits in the heart with 11C-PIB and PET. J Nucl Med 2013;54:213–20. [PubMed: 23238792]
26. Dorbala S, Vangala D, Semer J, et al. Imaging cardiac amyloidosis: a pilot study using (18)F-florbetapir positron emission tomography. Eur J Nucl Med Mol Imaging 2014;41:1652–62. [PubMed: 24841414]
27. Law WP, Wang WY, Moore PT, Mollee PN, Ng AC. Cardiac amyloid imaging with 18F-florbe-taben positron emission tomography: a pilot study. J Nucl Med 2016;1 Suppl:162. [PubMed: 27493273]
28. Biancalana M, Koide S. Molecular mechanism of thioflavin-T binding to amyloid fibrils. Biochim Biophys Acta 2010;1804:1405–12. [PubMed: 20399286]

Author Manuscript Author Manuscript Author Manuscript Author Manuscript

29. Biolo A, Ramamurthy S, Connors LH, et al. Matrix metalloproteinases and their tissue inhibitors in cardiac amyloidosis: relationship to structural, functional myocardial changes and to light chain amyloid deposition. Circ Heart Failure 2008;1:249–57. [PubMed: 19808299]
30. Banypersad SM, Sado DM, Flett AS, et al. Quantification of myocardial extracellular volume fraction in systemic AL amyloidosis: an equilibrium contrast cardiovascular magnetic resonance study. Circ Cardiovasc Imaging 2013;6:34–9. [PubMed: 23192846]
31. Kotecha T, Martinez-Naharro A, Treibel TA, et al. Myocardial edema and prognosis in amyloidosis. J Am Coll Cardiol 2018;71:2919–31. [PubMed: 29929616]
32. Fontana M, Banypersad SM, Treibel TA, et al. Differential myocyte responses in patients with cardiac transthyretin amyloidosis and light-chain amyloidosis: a cardiac MR imaging study. Radiology 2015:141744.
33. Quarta CC, Solomon SD, Uraizee I, et al. Left ventricular structure and function in transthyretin-related versus light-chain cardiac amyloidosis. Circulation 2014;129:1840–9. [PubMed: 24563469]
34. Brenner DA, Jain M, Pimentel DR, et al. Human amyloidogenic light chains directly impair cardiomyocyte function through an increase in cellular oxidant stress. Circ Res 2004;94:1008–10. [PubMed: 15044325]
35. Bhandari AK, Nanda NC. Myocardial texture characterization by two-dimensional echocardiography. Am J Cardiol 1983;51:817–25. [PubMed: 6829442]
36. Falk RH, Plehn JF, Deering T, et al. Sensitivity and specificity of the echocardiographic features of cardiac amyloidosis. Am J Cardiol 1987;59:418–22. [PubMed: 2949593]
37. Klein AL, Hatle LK, Burstow DJ, et al. Doppler characterization of left ventricular diastolic function in cardiac amyloidosis. J Am Coll Cardiol 1989;13:1017–26. [PubMed: 2647814]
38. Koyama J, Ray-Sequin PA, Davidoff R, Falk RH. Usefulness of pulsed tissue Doppler imaging for evaluating systolic and diastolic left ventricular function in patients with AL (primary) amyloidosis. Am J Cardiol 2002;89:1067–71. [PubMed: 11988197]
39. Milani P, Dispenzieri A, Scott CG, et al. Independent prognostic value of stroke volume index in patients with immunoglobulin light chain amyloidosis. Circ Cardiovasc Imaging 2018;11:e006588. [PubMed: 29752392]
40. Phelan D, Collier P, Thavendiranathan P, et al. Relative apical sparing of longitudinal strain using two-dimensional speckle-tracking echocardiography is both sensitive and specific for the diagnosis of cardiac amyloidosis. Heart 2012;98:1442–8. [PubMed: 22865865]
41. Sperry BW, Vranian MN, Tower-Rader A, et al. Regional variation in technetium pyrophosphate uptake in transthyretin cardiac amyloidosis and impact on mortality. J Am Coll Cardiol Img 2018;11:234–42.
42. Bravo PE, Fujikura K, Kijewski MF, et al. Relative apical sparing of myocardial longitudinal strain is explained by regional differences in total amyloid mass rather than the proportion of amyloid deposits. J Am Coll Cardiol Img 2019;12:1165–73.
43. Koyama J, Falk RH. Prognostic significance of strain Doppler imaging in light-chain amyloidosis. J Am Coll Cardiol Img 2010;3:333–42.
44. Senapati A, Sperry BW, Grodin JL, et al. Prognostic implication of relative regional strain ratio in cardiac amyloidosis. Heart 2016;102:748–54. [PubMed: 26830665]
45. Bellavia D, Pellikka PA, Dispenzieri A, et al. Comparison of right ventricular longitudinal strain imaging, tricuspid annular plane systolic excursion, and cardiac biomarkers for early diagnosis of cardiac involvement and risk stratification in primary systematic (AL) amyloidosis: a 5-year cohort study. Eur Heart J Cardiovasc Imaging 2012;13:680–9. [PubMed: 22307866]
46. Cappelli F, Porciani MC, Bergesio F, et al. Right ventricular function in AL amyloidosis: characteristics and prognostic implication. Eur Heart J Cardiovasc Imaging 2012;13:416–22. [PubMed: 22180463]
47. Patel AR, Dubrey SW, Mendes LA, et al. Right ventricular dilation in primary amyloidosis: an independent predictor of survival. Am J Cardiol 1997;80:486–92. [PubMed: 9285663]
48. de Gregorio C, Dattilo G, Casale M, Terrizzi A, Donato R, Di Bella G. Left atrial morphology, size and function in patients with transthyretin cardiac amyloidosis and primary hypertrophic cardiomyopathy- comparative strain imaging study. Circ J 2016;80:1830–7. [PubMed: 27350016]

Author Manuscript Author Manuscript Author Manuscript Author Manuscript

49. Nochioka K, Quarta CC, Claggett B, et al. Left atrial structure and function in cardiac amyloidosis. Eur Heart J Cardiovasc Imaging 2017;18:1128–37. [PubMed: 28637305]
50. White JA, Kim HW, Shah D, Fine N, et al. CMR imaging with rapid visual T1 assessment predicts mortality in patients suspected of cardiac amyloidosis. J Am Coll Cardiol Img 2014;7:143–56.
51. Syed IS, Glockner JF, Feng D, et al. Role of cardiac magnetic resonance imaging in the detection of cardiac amyloidosis. J Am Coll Cardiol Img 2010;3:155–64.
52. Fontana M, Pica S, Reant P, et al. Prognostic value of late gadolinium enhancement cardiovascular magnetic resonance in cardiac amyloidosis. Circulation 2015;132:1570–9. [PubMed: 26362631]
53. Zhao L, Tian Z, Fang Q. Diagnostic accuracy of cardiovascular magnetic resonance for patients with suspected cardiac amyloidosis: a systematic review and meta-analysis. BMC Cardiovasc Disorders 2016;16:129.
54. Fontana M, Banypersad SM, Treibel TA, et al. Native T1 mapping in transthyretin amyloidosis. J Am Coll Cardiol Img 2014;7:157–65.
55. Karamitsos TD, Piechnik SK, Banypersad SM, et al. Noncontrast T1 mapping for the diagnosis of cardiac amyloidosis. J Am Coll Cardiol Img 2013;6:488–97.
56. Banypersad SM, Fontana M, Maestrini V, et al. T1 mapping and survival in systemic light-chain amyloidosis. Eur Heart J 2015;36:244–51. [PubMed: 25411195]
57. Maceira AM, Prasad SK, Hawkins PN, Roughton M, Pennell DJ. Cardiovascular magnetic resonance and prognosis in cardiac amyloidosis. J Cardiovasc Magn Reson 2008;10:54. [PubMed: 19032744]
58. Fontana M, White SK, Banypersad SM, et al. Comparison of T1 mapping techniques for ECV quantification. Histological validation and reproducibility of ShMOLLI versus multibreath-hold T1 quantification equilibrium contrast CMR. J Cardiovasc Magn Res 2012;14:88.
59. Martinez-Naharro A, Abdel-Gadir A, Treibel TA, et al. CMR-verified regression of cardiac AL amyloid after chemotherapy. J Am Coll Cardiol Img 2018;11:152–4.
60. Mongeon FP, Jerosch-Herold M, Coelho-Filho OR, Blankstein R, Falk RH, Kwong RY. Quantification of extracellular matrix expansion by CMR in infiltrative heart disease. J Am Coll Cardiol Img 2012;5:897–907.
61. Giri S, Chung YC, Merchant A, et al. T2 quantification for improved detection of myocardial edema. J Cardiovasc Magn Reson 2009;11:56. [PubMed: 20042111]
62. Perugini E, Guidalotti PL, Salvi F, et al. Noninvasive etiologic diagnosis of cardiac amyloidosis using 99mTc-3,3-diphosphono-1,2-propanodicarboxylic acid scintigraphy. J Am Coll Cardiol 2005;46:1076–84. [PubMed: 16168294]
63. Bennani Smires Y, Victor G, Ribes D, et al. Pilot study for left ventricular imaging phenotype of patients over 65 years old with heart failure and preserved ejection fraction: the high prevalence of amyloid cardiomyopathy. Int J Cardiovasc Imaging 2016;32:1403–13. [PubMed: 27240600]
64. Castano A, Haq M, Narotsky DL, Goldsmith J, et al. Multicenter study of planar technetium 99m pyrophosphate cardiac imaging: predicting survival for patients with ATTR cardiac amyloidosis. JAMA Cardiol 2016;1:880–9. [PubMed: 27557400]
65. Hutt DF, Fontana M, Burniston M, et al. Prognostic utility of the Perugini grading of 99mTc-DPD scintigraphy in transthyretin (ATTR) amyloidosis and its relationship with skeletal muscle and soft tissue amyloid. Eur Heart J Cardiovasc Imaging 2017;18:1344–50. [PubMed: 28159995]
66. Wagner T, Page J, Burniston M, et al. Extracardiac (18)F-florbetapir imaging in patients with systemic amyloidosis: more than hearts and minds. Eur J Nuclear Med Mol Imaging 2018;45:1129–38.
67. Osborne DR, Acuff SN, Stuckey A, Wall J. A routine PET/CT protocol with simple calculations for assessing cardiac amyloid using 18F-Florbetapir. Front Cardiovasc Med 2015;2:23. [PubMed: 26664895]
68. Lee SP, Lee ES, Choi H, et al. (11)C-Pittsburgh B PET imaging in cardiac amyloidosis. J Am Coll Cardiol Img 2015;8:50–9.
69. Pilebro B, Arvidsson S, Lindqvist P, et al. Positron emission tomography (PET) utilizing Pittsburgh compound B (PIB) for detection of amyloid heart deposits in hereditary transthyretin amyloidosis (ATTR). J Nucl Cardiol 2018;25:240–8. [PubMed: 27645889]

Author Manuscript Author Manuscript Author Manuscript Author Manuscript

70. Lin KJ, Hsu WC, Hsiao IT, et al. Whole-body biodistribution and brain PET imaging with [18F]AV-45, a novel amyloid imaging agent-a pilot study. Nucl Med Biol 2010;37:497–508. [PubMed: 20447562]

71. Park MA, Padera RF, Belanger A, et al. 18F-Florbetapir binds specifically to myocardial light chain and transthyretin amyloid deposits: autoradiography study. Circulation Cardiovasc Imaging 2015;8.

72. Ezawa N, Katoh N, Oguchi K, Yoshinaga T, Yazaki M, Sekijima Y. Visualization of multiple organ amyloid involvement in systemic amyloidosis using ^{11}C-PiB PET imaging. Eur J Nuclear Med Mol Imaging 2018;45:452–61.

73. Gilstrap LG, Dominici F, Wang Y, et al. Epidemiology of cardiac amyloidosis-associated heart failure hospitalizations among fee-for-service Medicare beneficiaries in the United States. Circ Heart Fail 2019;12:e005407. [PubMed: 31170802]

74. Salinaro F, Meier-Ewert HK, Miller EJ, et al. Longitudinal systolic strain, cardiac function improvement, and survival following treatment of light-chain (AL) cardiac amyloidosis. Eur Heart J Cardiovasc Imaging 2017;18:1057–64. [PubMed: 27965280]

75. Solomon SD, Adams D, Kristen AV, et al. Effects of Patisiran, an RNA interference therapeutic, on cardiac parameters in patients with hereditary transthyretin-mediated amyloidosis: an analysis of the APOLLO Study. Circulation 2019;139:431–43. [PubMed: 30586695]

76. Castano A, DeLuca A, Weinberg R, et al. Serial scanning with technetium pyrophosphate (^{99m}Tc-PYP) in advanced ATTR cardiac amyloidosis. J Nucl Cardiol 2016;23:1355–63. [PubMed: 26453570]

Author Manuscript Author Manuscript Author Manuscript Author Manuscript

HIGHLIGHTS

- Cardiac amyloidosis is substantially underdiagnosed and AL amyloidosis, if untreated, is rapidly fatal. Emerging therapies for cardiac amyloidosis increase the urgency for developing noninvasive imaging for early detection and for tracking therapeutic response.
- Classic imaging features on echocardiography and cardiac magnetic resonance, although typical for cardiac amyloidosis, are not specific enough to distinguish light chain amyloidosis from transthyretin amyloidosis.
- Myocardial bone-avid radiotracer uptake is highly specific for transthyretin cardiac amyloidosis when plasma cell dyscrasia has been excluded; it is now replacing the need for biopsy in many patients.
- Detection of early cardiac amyloidosis, quantitation of its burden, and assessment of response to therapy are important next steps for imaging to advance the evaluation and management of cardiac amyloidosis.

Author Manuscript Author Manuscript Author Manuscript Author Manuscript

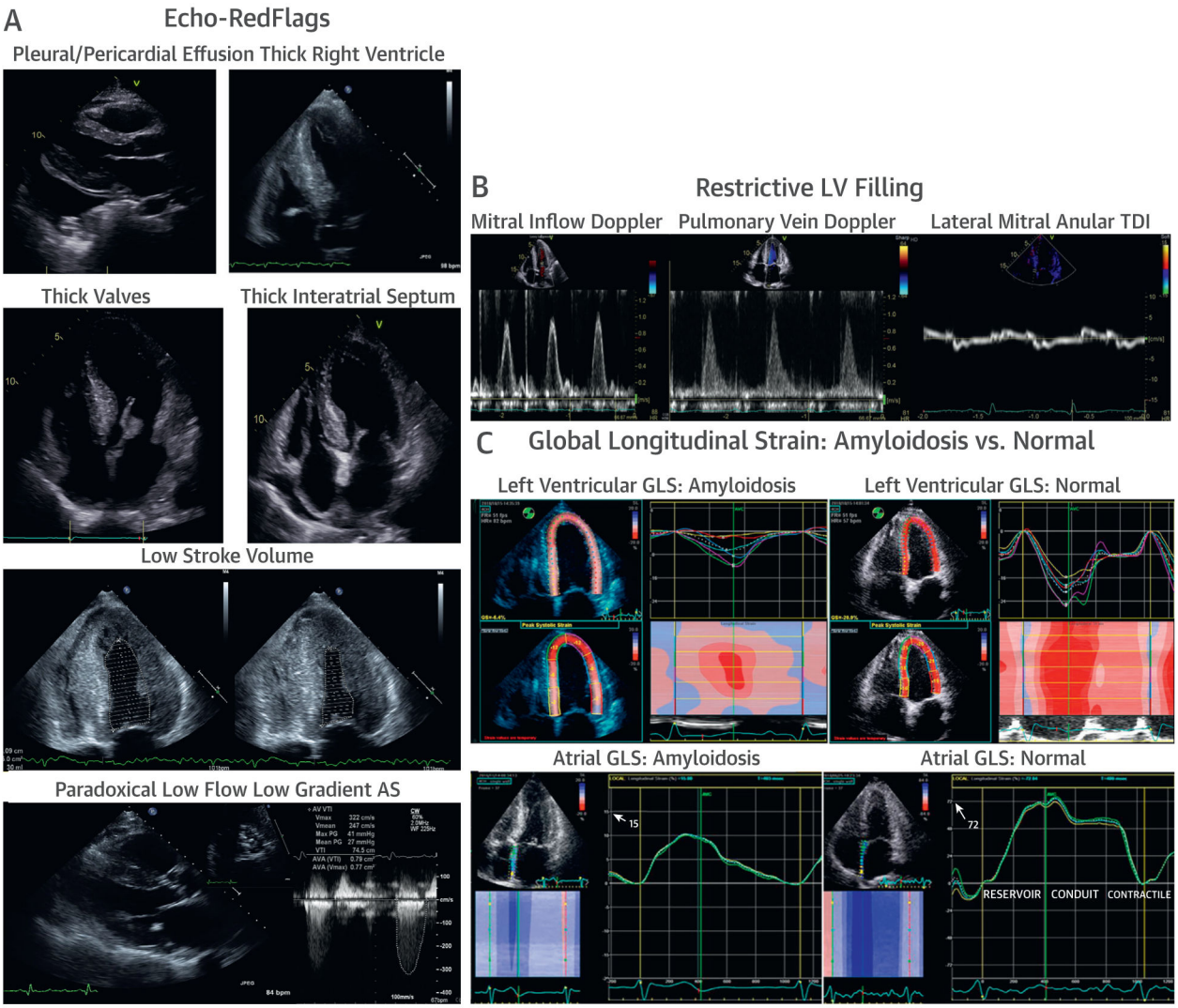

FIGURE 1. Echocardiography in CA

In the context of a thick Left ventricle (LV), the following features should be considered red flags for cardiac amyloidosis (CA): **(A)** pericardial and/or pleural effusions, thick right ventricle, thick valves, thick interatrial septum, small LV cavity size with low stroke volume, and paradoxical low flow, low gradient aortic stenosis. **(B)** Advanced CA results in restrictive LV filling patterns with rapid E-wave deceleration time, a predominant S wave on pulmonary venous Doppler, and low myocardial relaxation velocities on tissue Doppler imaging (TDI) at the mitral annulus. Finally, amyloid infiltration impairs **(C)** global Longitudinal strain (GLS) characteristically with apical sparing of the LV apex, in contrast to a normal pattern, and severely reduced contractile function of the atrial myocardium, in contrast to a normal pattern.

AS = aortic stenosis.

Author Manuscript Author Manuscript Author Manuscript Author Manuscript

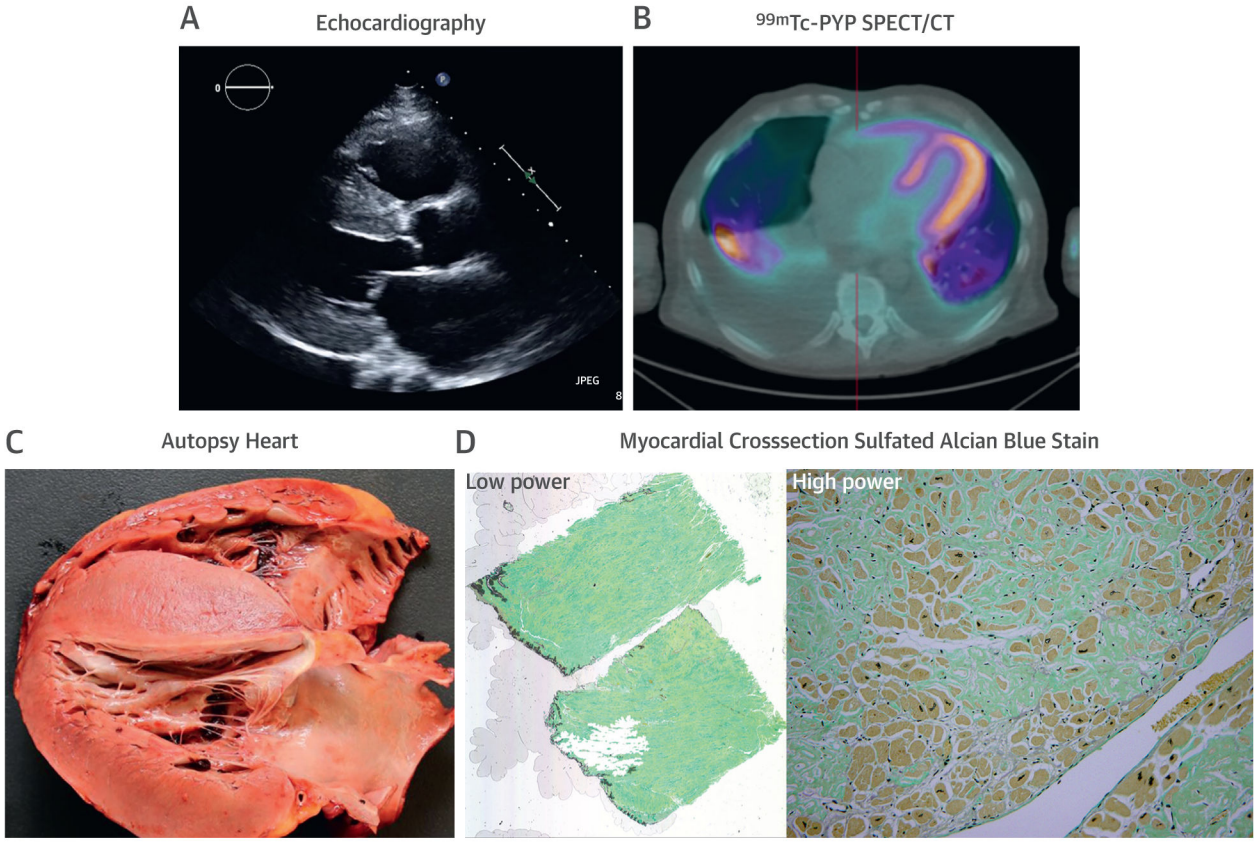

Figure 2. Cardiac Structural Changes Typically Indicate Advanced CA

Images of a 54-year-old African American man with heart failure who eventually succumbed to sepsis. (A) Echocardiogram, **(B)** technetium-99m (Tc-99m) -pyrophosphate (PYP) single-photon emission computed tomography/computed tomography (SPECT/CT) (strongly positive, grade 3 uptake), and **(C)** autopsy images are shown. A plasma cell dyscrasia was excluded, and genetic testing revealed a TTR gene mutation (*Asp18Asn*). Autopsy confirmed substantial transmural and diffuse amyloid deposition. **(D)** Low- and high-power sulfated Alcian Blue stain with **blue/green** staining amyloid and **yellow/brown** staining myocytes. Autopsy and histology images courtesy of Dr. Robert E. Padera. Abbreviation as in Figure 1.

Author Manuscript Author Manuscript Author Manuscript Author Manuscript

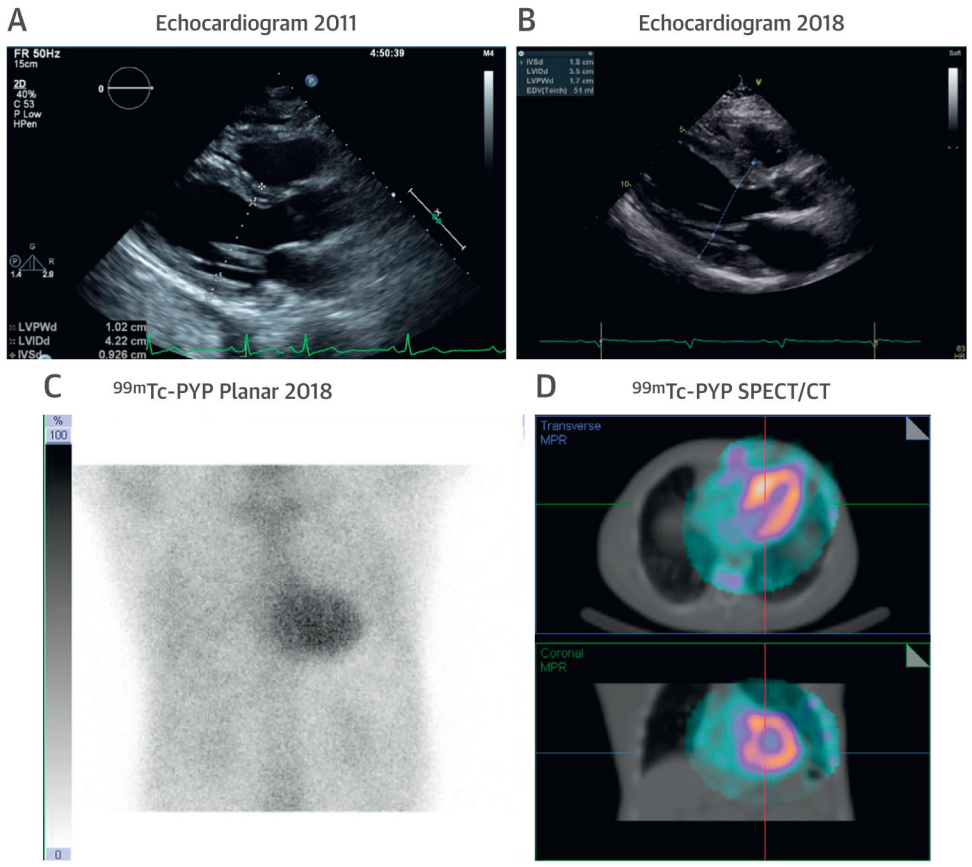

FIGURE 3. A High Clinical Suspicion of ATTR CA Is Needed in Older Persons With Hypertension and Increased LV wall Thickness

Images of a 76-year-old man with a history of hypertension and progressive increase in LV wall thickness from **(A)** 10 mm in 2011 to **(B)** 18 mm in 2018. His cardiologist questioned whether this could be explained solely on the basis of hypertension. Echocardiography also revealed right ventricular wall thickening, raising the possibility of transthyretin (ATTR) CA. Serum and urine immunofixation studies and serum light chain levels were normal. **(C and D)** A Tc-99-PYP scan revealed grade 3 myocardial uptake, confirming ATTR CA. Abbreviations as in Figures 1 and 2.

Author Manuscript Author Manuscript Author Manuscript Author Manuscript

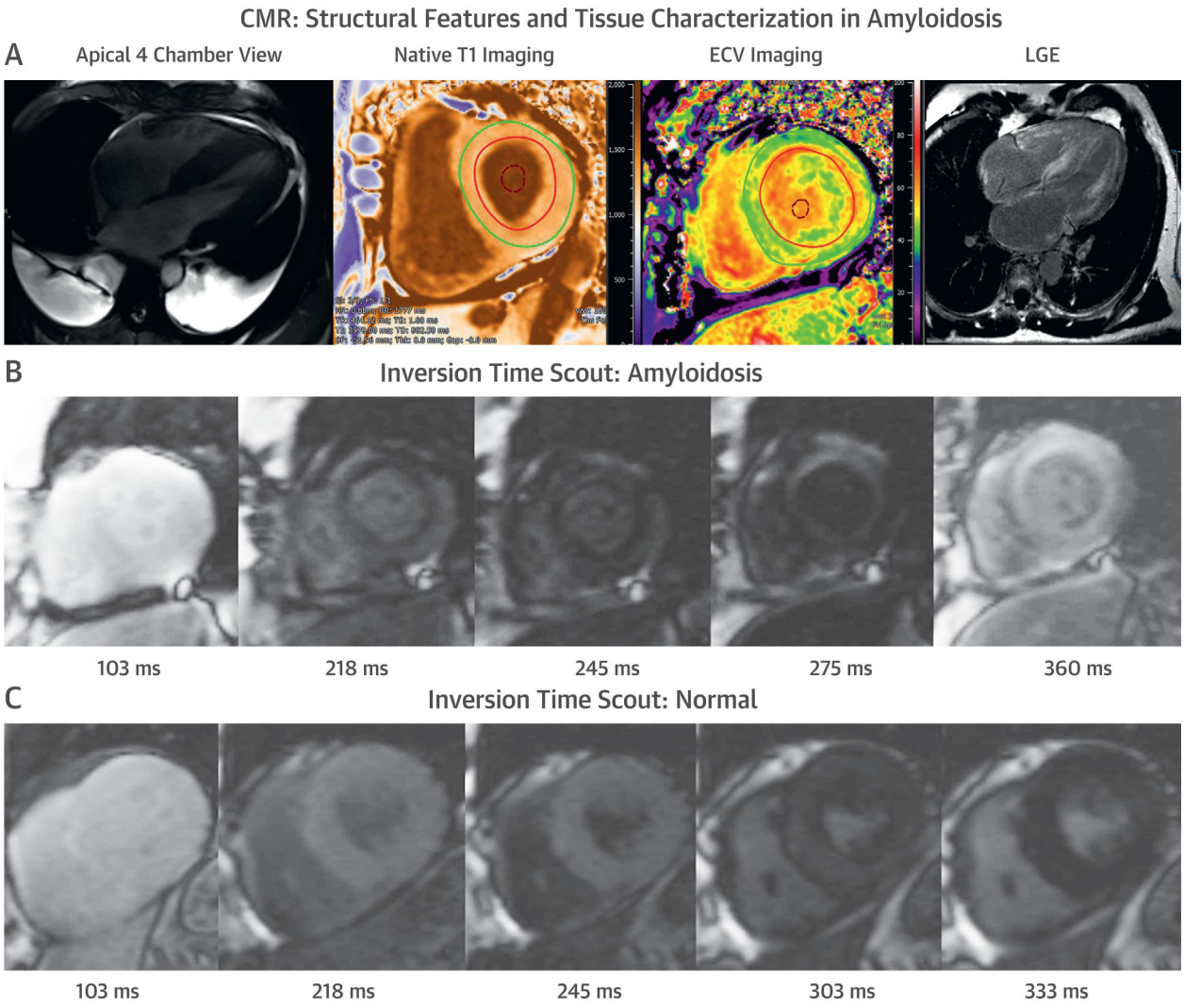

FIGURE 4. CMR in CA

Cardiovascular magnetic resonance (CMR) provides characteristic imaging of the **(A)** structural changes and (B) powerful tissue characterization with features of high native T1, expanded extracellular volume (ECV), and late gadolinium enhancement (LGE) (diffuse, subendocardial, or transmural). **(C)** Post-gadolinium myocardial signal intensity changes characteristically with myocardial signal nulling before the blood pool signal in amyloidosis and vice versa in non-amyloid hearts. Abbreviation as in Figure 1.

Author Manuscript Author Manuscript Author Manuscript Author Manuscript

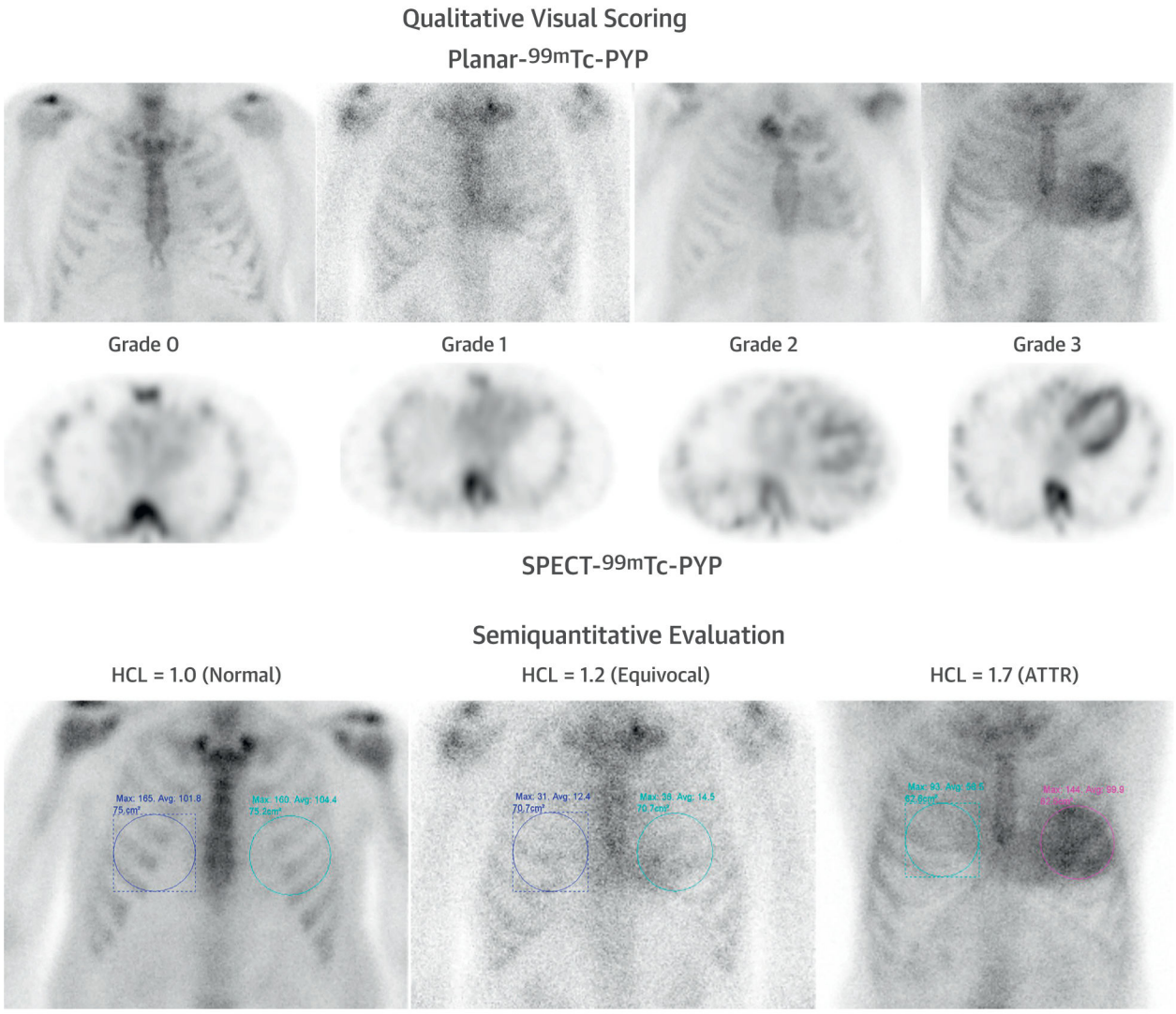

FIGURE 5. Tc-99m–PYP in CA

Tc-99m –PYP planar and SPECT scans graded visually (grade 0, negative, to grade 3, strongly positive) and semi-quantitatively using the heart to contralateral lung uptake (HCL) ratio (normal, equivocal and diagnostic of ATTR). Abbreviations as in Figures 1 to 3.

Author Manuscript Author Manuscript Author Manuscript Author Manuscript

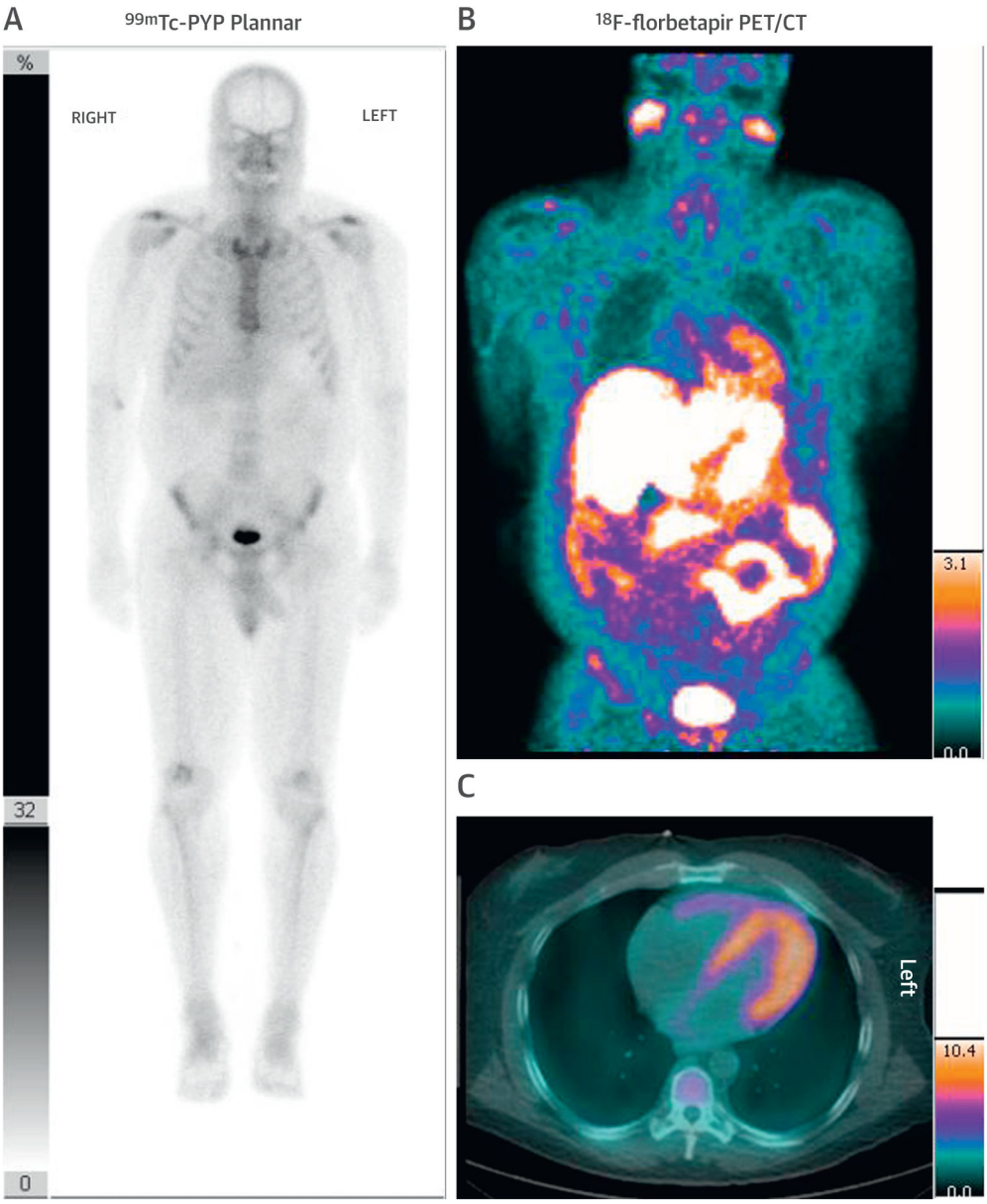

FIGURE 6. A Negative Tc-99m–PYP Does Not Exclude CA

A 56-year-old African American man with a V122I TTR mutation presented with heart failure and an echocardiogram suspicious for CA. **(A)** A Tc-99m–PYP scan revealed grade 1 uptake (myocardial uptake less than rib uptake). Serum and urine immunofixation and serum light chain assay suggested light chain (AL) amyloidosis. An endomyocardial biopsy with mass spectroscopy confirmed Lambda AL CA. **(B)** Cardiac and partial whole body F-18-florbetapir positron emission tomography (PET/CT) images, as part of a research protocol, demonstrated intense myocardial and parotid uptake of F-18-florbetapir. He received a regimen of bortezomib, cyclophosphamide, and dexamethasone with complete hematological response. Abbreviations as in Figures 1 and 2.

Author Manuscript Author Manuscript Author Manuscript Author Manuscript

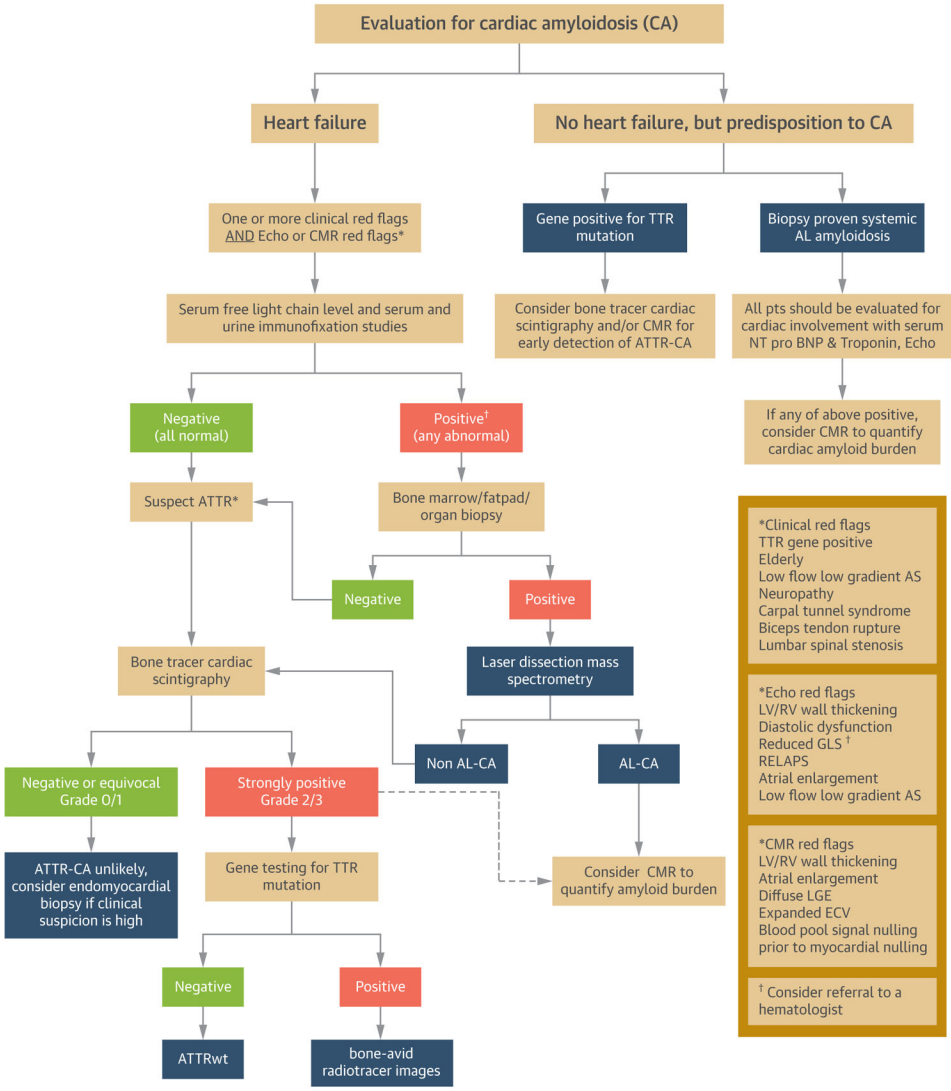

Figure 7. An Algorithmic Approach to Imaging-Based Evaluation of CA

CA may be considered in patients with heart failure as well as in patients without heart failure but with a predisposition to CA. MGUS = monoclonal gammopathy of uncertain significance; Pts = patients; other abbreviation as in Figure 1.

Author Manuscript Author Manuscript Author Manuscript Author Manuscript

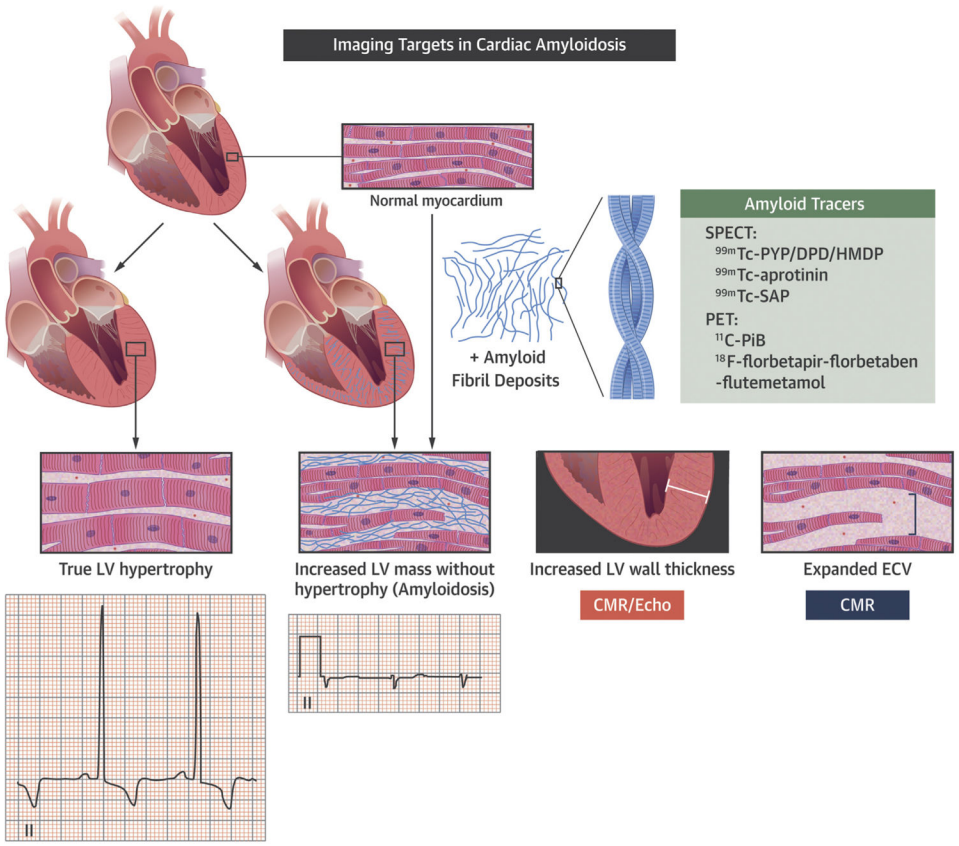

CENTRAL ILLUSTRATION. Imaging Targets in Cardiac Amyloidosis

Interstitial amyloid deposits **(purple)** thicken the myocardium and expand ECV; but, these features or voltage on electrocardiography cannot definitively distinguish infiltration from true myocardial hypertrophy. Targeted amyloid imaging with radiotracers are specific to image myocardial amyloid deposits. CMR = cardiac magnetic resonance; DPD = -3,3-diphosphono-1,2 propanodicarboxylic acid; ECV=extracellular volume; HMDP = hydroxymethylene diphosphonate; PiB = Pittsburgh B compound; PYP = pyrophosphate; SAP = serum amyloid P component; ^{99m}Tc = technetium-99m.